ELSEVIER

Global and Planetary Change 12 (1996) 119–133

GLOBAL AND PLANETARY CHANGE

Quantification of the Pliocene–Pleistocene erosion of the Barents Sea from present-day bathymetry

Eigil Rasmussen [a], Willy Fjeldskaar [b,*]

[a] Norsk Hydro, P.O. Box 200, 1321 Stabekk, Norway
[b] RF-Rogaland Research, P.O.Box 2503, 4004 Stavanger, Norway

Received 14 December 1994; accepted 4 May 1995

Abstract

We present an attempt to quantify the Tertiary and Quaternary erosion on the Barents Shelf in a two step model. The first step is a tectonically related uplift in the order of 500–2000 m of the NW Barents Shelf in the Early Tertiary with subsequent erosion in the Eocene–Miocene period and transport of 950,000 km^3 of erosional products to the sedimentary basins on the southern and eastern Barents shelf and to the continental margins to west and north. The second step involves a regional glacial erosion in Pliocene–Pleistocene times with removal of 1,280,000 km^3 of sediments that today are located in wedges along the western and northern Barents Shelf margins.

With the present-day topography and bathymetry, the preglacial relief is reconstructed and used to calculate the glacial erosion by isostatic modelling. The results indicate that the total erosion increases from 500–700 m in the Southern Barents Sea, to an excess of 2000 m in a zone from Spitsbergen to Franz Josephs Land. Planimetering of this erosional map gives a total of 1,200,000 km^3 of eroded material, which agrees with the estimated 1,280,000 km^3 of material in the sedimentary wedges along the western and northern Barents Shelf Margin.

1. Introduction

From the first exploration wells were drilled on the Barents Shelf in 1981, it has become clear to petroleum explorers that the shelf area has been subject to extensive erosion in Tertiary to Quaternary times. These conclusions are based on results from studies of diagenesis, maturation of source rocks, compaction of shale and using various other methods (Nyland et al., 1992). Also on Svalbard, significant erosion is documented to have occurred in Tertiary times (Manum and Throndsen, 1978). Regional mapping in the mid 1980s located the erosional products in sedimentary wedges along the western and northern margin of the Barents Shelf (Nøttvedt et al., 1988)

The age of the erosion has been subject to considerable discussion. In a re-dating study presented by Eidvin and Riis (1989) a late Pliocene to Pleistocene age was proposed for 2/3 of the wedge volumes located along the present day western shelf margin. For a detailed age-discussion of the Tertiary sediments along the Western Barents Sea Margin, see Fiedler and Faleide (1996) and Faleide et al. (1996).

* Corresponding author.

0921-8181/96/$15.00
SSDI 0921-8181(95)00015-1

These young age-datings for most of the sediment volumes immediately led to glacial erosion being proposed as the major mechanism for the removal of sediments on the whole shelf area, with transportation and deposition of erosional products in the wedges located along the shelf (Vorren et al., 1989), although the detailed erosional mechanisms still are debatable. Large volumes of Early Tertiary sediments are also preserved in wedges along the continental shelf and in the sedimentary basins on the south-western Barents shelf, indicating that a considerably erosion also occurred in Early Tertiary times (Rasmussen et al., in press).

In the present study we therefore divide the Tertiary erosional history of the Barents Shelf into the two different episodes:

—an Early Tertiary phase after continental rifting in North Atlantic involving tectonic uplift of the whole north-western Barents Shelf with subsequent sub aerial erosion and deposition of erosional products along the shelf margins and filling of sedimentary basins on the southern and south-eastern Barents Shelf,

—a second episode of latest Tertiary and Quaternary age characterised by glacial erosion on the whole shelf area with transport of erosional products to the present day margins, and with subsequent isostatic uplift of the eroded shelf area.

In this paper we focus mainly on the last episode. Together with realistic geological assumptions to reconstruct the pre-glacial relief, we will use the present-day bathymetry and topography on the Barents Shelf aided by isostatic modelling to quantify the glacial erosion. Mapping of the volume of the erosional products along the present-day margins is used to constrain the erosional estimates.

2. Erosion and isostasy

Erosion in the Barents Sea will result in isostatic uplift of the effectively elastic lithosphere to compensate for the loss of the sedimentary mass. The relaxation time for the isostatic compensation estimated from the post-glacial uplift is only a few thousand years (Fjeldskaar and Cathles, 1991). Thus it is reasonable to assume that the flexural equilibrium was achieved during the erosional process. The time period considered here, less than 5 million years, is, however, too short to require taking the viscous properties of the lithosphere into account (as described in Fjeldskaar and Pallesen, 1989).

In this paper we are interested in the accumulated effect of all glaciations in the area. We assume that the pre-Quaternary surface was at sea level and that the eroded Pre-Quaternary sediment has been replaced by Quaternary sediment and sea water. Assuming local isostatic compensation (effective elastic thickness = 0) the relation between present day water depth (H), thickness of the Quaternary sediment (Q), change in the relief in Pliocene–Pleistocene time (DR) and the amount of erosion (S) is:

$$S = \frac{H(\rho_m - \rho_w) + Q(\rho_m - \rho_q) + \Delta R \cdot \rho_m}{(\rho_m - \rho_s)} \qquad (1)$$

where ρ_m, ρ_w, ρ_q and ρ_s is the density of the mantle, sea water, Quaternary sediment and eroded sediments, respectively.

3. Earth model

If a load (positive or negative) is applied to the elastic lithosphere covering the asthenosphere, part of the applied load will be supported by shear stress in the lithosphere, part by the buoyant forces of the asthenosphere beneath acting through the lithosphere. Loads of short wavelength are supported by the lithosphere so that the lithosphere acts as a lowpass filter. The characteristics of this filter depends on the elastic strength of the lithosphere, parameterized by the flexural rigidity (D). The relationship between the effective elastic thickness t_e of the lithosphere and the flexural rigidity D is given by the formula:

$$D = Et_e^3/12(1 - \upsilon^2)$$

where ν is Poisson's ratio and E is Young's modulus.

For a flat earth approximation with a uniformly thick elastic lithosphere the regional isostatic compensation can be calculated using the Fourier transforms. The method used here is described in detail in Cathles (1975) and Fjeldskaar and Cathles (1991). In the Fourier domain Eq. 1 becomes with the introduction of an elastic lithosphere:

$$S(k_x,k_y) = \frac{H(k_x,k_y)(\rho_m - \rho_w) + Q(k_x,k_y)(\rho_m - \rho_q) + \Delta R(k_x,k_y)\rho_m}{\alpha(k_x,k_y)(\rho_m - \rho_s)} \quad (2)$$

where k_x, k_y $(= 2n/\lambda_y)$ are the wave-numbers and $\alpha(k_x, k_y)$ is the "lithosphere filter":

$$\alpha(k_x,k_y) = 1 + \frac{k^4}{\rho_m g} D(k_X,k_Y)$$

where:

$$k = \sqrt{k_x^2 + k_y^2}$$

4. Flexural rigidity

The influence of the lithosphere in isostatic movements has been subject of much debate. It is now accepted that the lithosphere behaves like an elastic plate overlying a viscous fluid. This concept is, however, not new. Smoluchowski (1909) explained

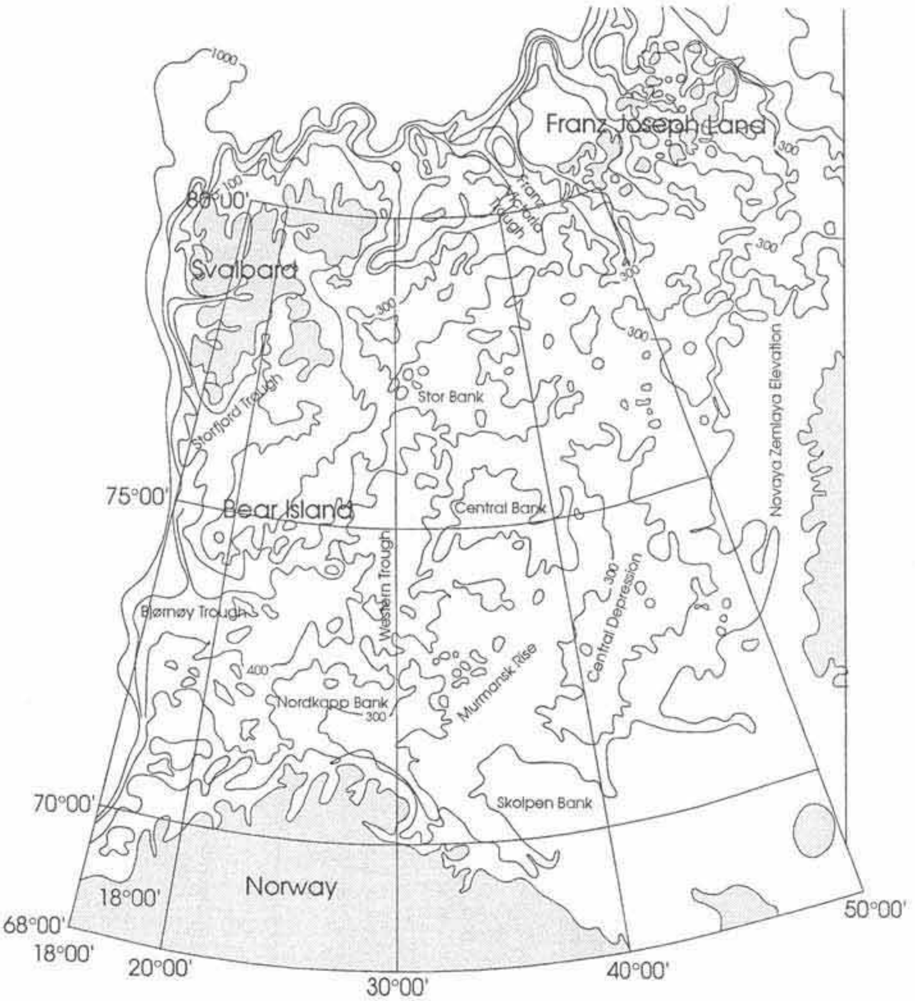

Fig. 1. Simplified bathymetry of the Barents Sea.

the folding in synclinal fold belts by buckling of the elastic lithosphere. The flexure and its gravity effect at passive continental margins was studied by Gunn (1943, Gunn (1944). Jeffreys (1959) studied the deformation of an elastic crust by bending of a thin elastic sheet. The approach to including the lithosphere in isostatic adjustment calculations was pioneered by Brotchie and Silvester (1969) and Walcott (1970). Brotchie and Silvester (1969) investigated the influence of a load on its neighbouring regions caused by the rigidity of the lithosphere. Based on long-term isostatic adjustment of small scale loads at various locations on the globe, Walcott (1970) concluded the flexural rigidity of the lithosphere ranged from 5×10^{22} to 4×10^{24} Nm, but the flexural rigidity over short timescales could be larger ($6–9 \times 10^{24}$ Nm). Gravity anomalies reflecting long term load support in Fennoscandia suggest a flexural rigidity of between 1 and 5×10^{24} Nm (Cathles, 1975). The flexure of the Pacific plate under the loading of the Hawaiian–Emperor chain was studied by Watts (1978). His results suggest there is a systematic increase in the thickness of the elastic lithosphere with age. These results seem to be consistent with the results from flexure at ocean trenches, based on the width of the forebulge (Caldwell and Turcotte, 1979).

The response of ice-load redistribution on earth models with various lithospheric thicknesses is calculated to determine the elastic lithosphere rheology of Fennoscandia. Assuming a uniform lithosphere, the uplift data of Fennoscandia suggest that the flexural rigidity is equal to or less than 10^{24} Nm, corresponding to an effective elastic thickness of approximately 50 km (Fjeldskaar and Cathles, 1991). This is assumed to be an upper bound of the earth's rigidity because the ice model used in that study has minimum extent and maximum ice surface profile.

Isostatic and tectonic modelling in sedimentary basins in the North Sea has also given estimates of the elastic thickness of the lithosphere. Barton and Wood (1984) suggested a 5 km elastic lithosphere thickness for the North Sea. This is in accordance with the suggestion of Fjeldskaar et al. (1993) that the flexural rigidity of the lithosphere in the Egersund Basin, North Sea, is less than 10^{22} Nm ($t_e \leq 10$ km).

In the Barents Sea, however, D is not well constrained. We have, therefore, used three different values of the flexural rigidity, 0.1, 1.0 and 10×10^{23} Nm ($t_e \approx 10$, 25 and 50 km, respectively).

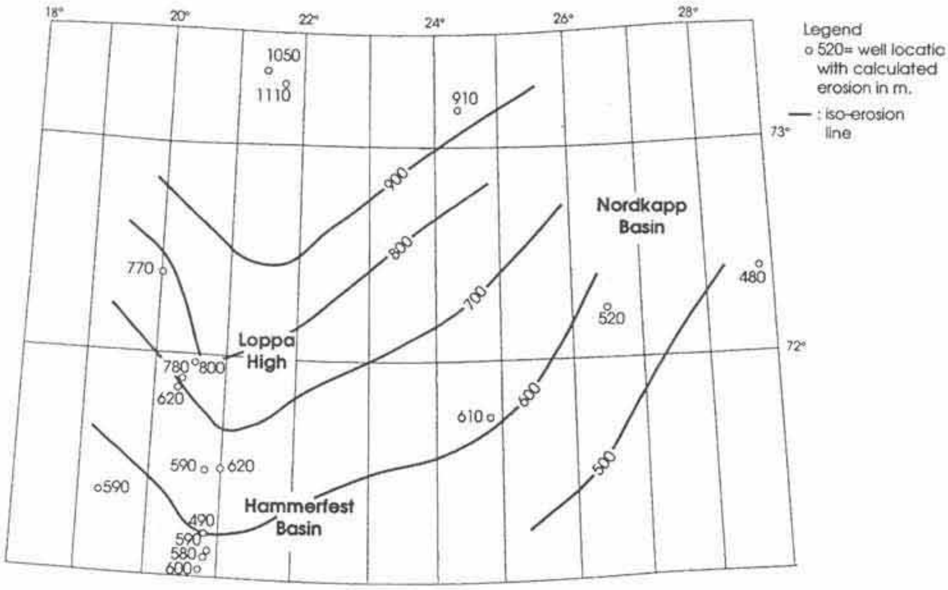

Fig. 2. Estimated Pliocene–Pleistocene erosion on the southern Barents Sea based on parameters from exploration wells.

5. Calculated erosion

A number of bathymetric troughs are observed to cut the Barents Shelf Fig. 1, and drain across the continental shelf where large volumes of anticipated erosional products are located (Nøttvedt et al., 1988; Nyland et al., 1992). In a number of papers the bathymetry on the southern shelf has been explained as a result of glacial erosion (Vorren et al., 1989), a model which is accepted here.

Based on the earth model above and Eq. 1 we calculated the eroded material as a function of the present day bathymetry and the thickness of the Quaternary sediments. The density parameters are tabulated in Table 1, and are based on observations from exploration wells in the area. It is also assumed that the preglacial water depth on the southern Barents Shelf was close to 0 m, due to infill of basins resulting from the erosion of the NW uplifted Barents Shelf. Fig. 2 displays the erosion estimates based on parameters as observed in exploration wells on the southern Barents Shelf. In the southern Barents Sea the erosion is seen to increase from 500–600

Table 1
Parameter values used in the calculations

Poisson's ratio	$\upsilon = 0.25$
Young's modulus	$E = 10.3 \times 10^{10}\ \mathrm{Nm}^{-2}$
Density of mantle	$\rho_m = 3300\ \mathrm{kg/m^3}$
Density of Quaternary sediments	$\rho_q = 1900\ \mathrm{kg/m^3}$
Density of eroded sediments	$\rho_s = 2200\ \mathrm{kg/m^3}$
Water density	$\rho_w = 1000\ \mathrm{kg/m^3}$
Magnitude of compression	$N = 1.0 \times 10^{13}\ \mathrm{Nm}^{-1}$

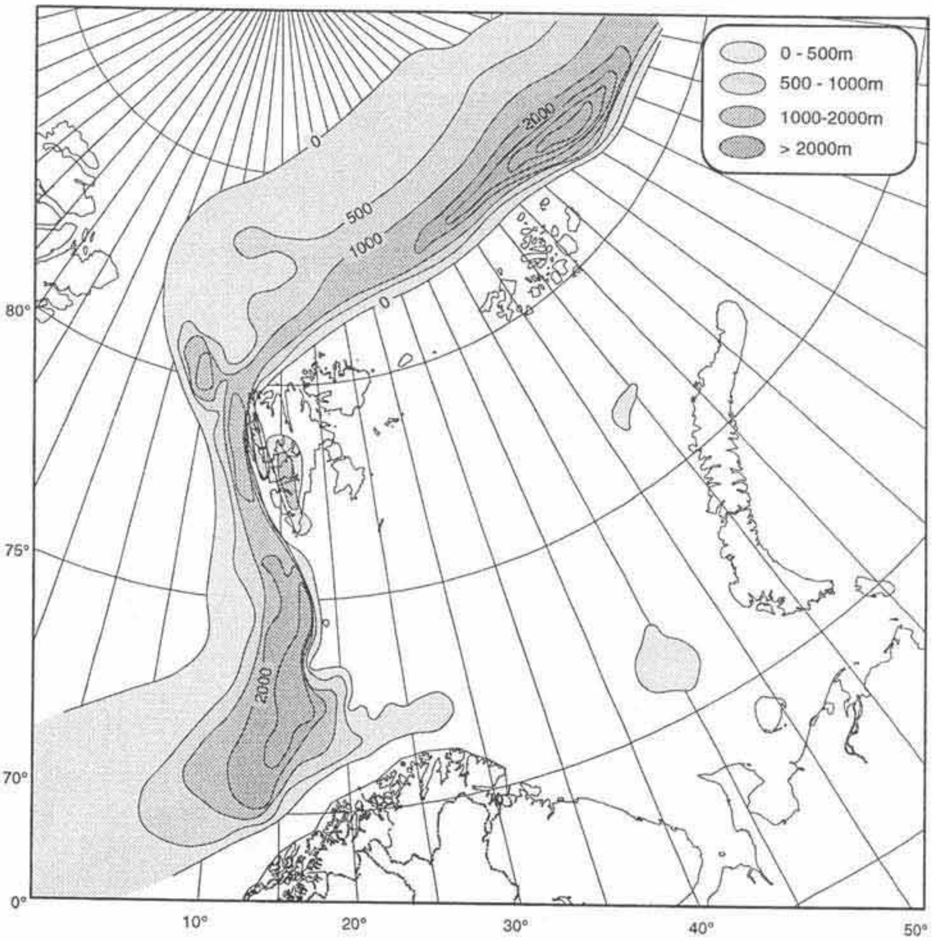

Fig. 3. Paleocene–Miocene sediment thicknesses on the Barents Shelf and margins.

m in Hammerfest–Nordkapp Basins, to in excess of 900–1000 m north of the Loppa High. A gradually lower erosion to less than 500 m is anticipated for the south-eastern Barents Shelf.

The erosion estimates mimic to a large extent the bathymetry, only slightly modified by the variations in Quaternary thicknesses. The difference between the flexural method and the local isostatic approximation could be significant in local areas. In general, however, the difference is less than 100 m.

For the NW Barents Shelf where a preglacial elevation above sea level is anticipated (see discussion below), a coarse preglacial relief must be established before isostatic models can be applied.

6. Mapping of erosional volumes

One way to reconstruct the preglacial relief on the Barents Shelf is to map the volume of Pliocene–Pleistocene erosional products along the present day margin, spread them back to their provenance area—already knowing the erosion on the southern Barents Shelf (Fig. 2)—and correct for the isostatic adjustment to a different mass distribution.

Fig. 3 displays the isopach map of the Base Tertiary to Miocene sedimentary thickness along the western and northern margin of the Barents Shelf, while the isopach of the Pliocene to Pleistocene is displayed in Fig. 4. In the west, the mapping is based

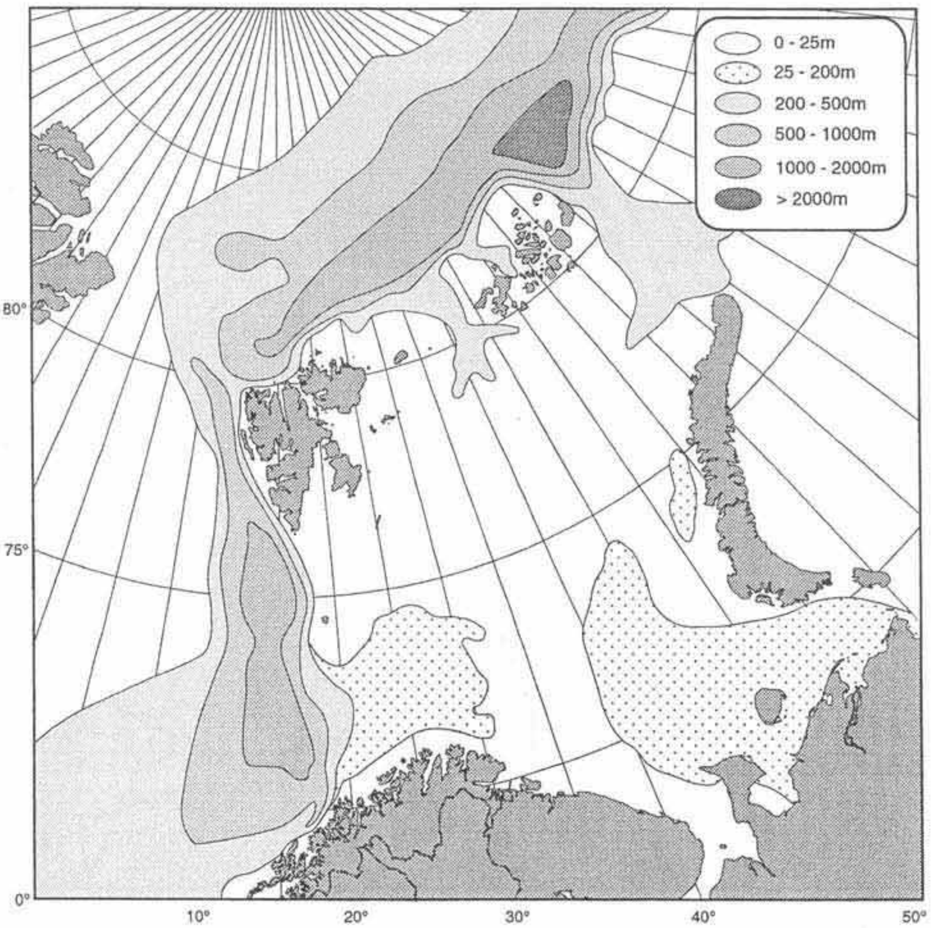

Fig. 4. Pliocene–Pleistocene sediment thicknesses on the Barents Shelf and margins.

mostly on seismic data available to the oil industry, which makes the volume estimates reliable. Volume calculations along the western margin gives a total of 280,000 km^3 of Early Tertiary to Miocene sediments, and an additional 530,000 km^3 of Pliocene to Pleistocene sediments.

To the north of the Barents Shelf the database is very scarce, with few available seismic lines. In our approach, we have based our isopachs on a literature synthesis where several attempts have been made to map the whole sedimentary wedge by using different methods (Kristoffersen, 1990; Vågnes, 1996). In addition we have used unpublished Russian data to support our calculations. The total Tertiary to Quaternary sediment volume is estimated to be 1,100,000 km^3, but it is noted that considerably uncertainty exist with regard to this estimate. For further division we have divided the volumes in the same proportions as empirically observed on the western Barents Shelf, with approximately 2/3 of the volume in the Pliocene–Pleistocene wedge, and 1/3 in the Early Tertiary to Miocene wedge. The results gives very coarse estimates of 350,000 km^3 sediments, localised in the Early Tertiary to Miocene wedge, and 750,000 km^3 in the Pliocene–Pleistocene wedge, stretching from Svalbard to east of Franz Joseph Land.

For most of the southern Barents Shelf, Late Cretaceous to Early Tertiary sediments are today subcropping on the sea bottom (NPD subcrop map). This implies that a large proportion of the eroded sediments in this area were Tertiary sedimentary rocks. By using seismic extrapolation methods and our estimated erosional thicknesses as shown in Fig. 2, the preglacial extension of the Tertiary deposits on

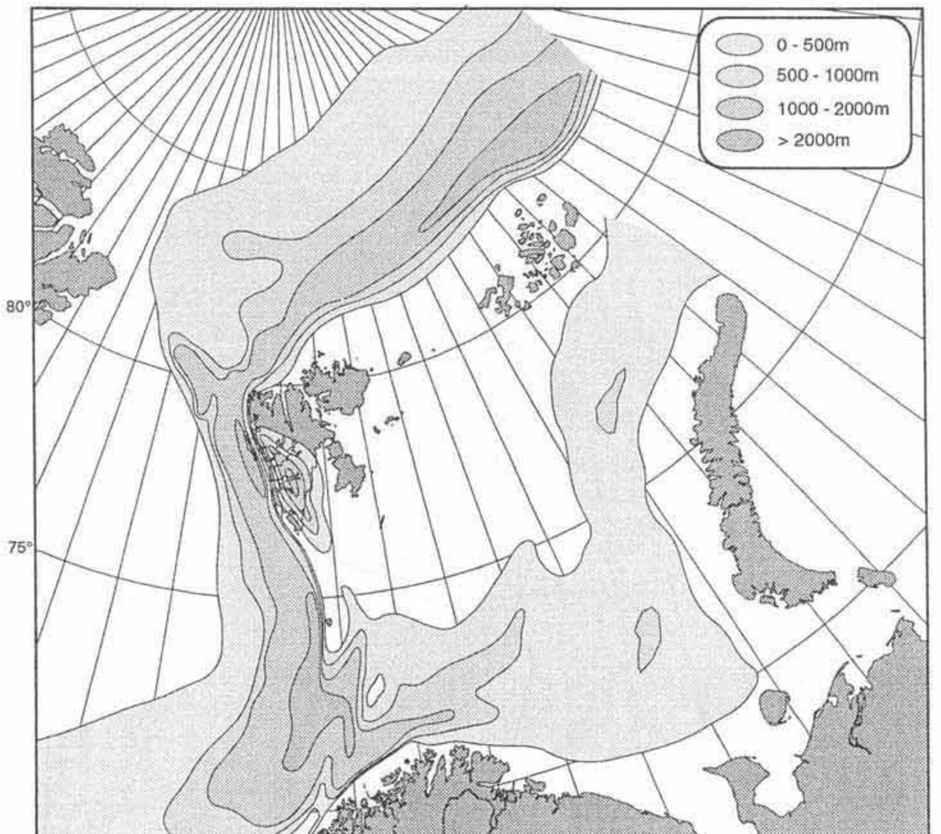

Fig. 5. Reconstructed preglacial Paleocene–Miocene sediment thicknesses on the Barents Shelf and margins.

the southern and southeastern Barents Shelf is reconstructed in Fig. 5. These volumes of sediments are believed to derive from provenance areas on the northwestern tectonically uplifted shelf, possibly with a minor contribution also from the Fennoscandian and Uralian areas.

Based on the map in Fig. 5 the Tertiary sediments located on the southern and southeastern Barents shelf—which later is to be eroded by glacial erosion —is calculated to amount to 320,000 km^3. Including this sediment volume the total volumes of Early Tertiary to Miocene erosional products add up to 950,000 km^3 (280,000 km^3 in basins along the western shelf, 350,000 km^3 north of the shelf, and 320,000 km^3 deposited and later eroded from the southern and eastern shelf). In addition a volume of 1,280,000 km^3 of Pliocene–Pleistocene erosional products are observed along the western and northern shelf areas (530,000 km^3 and 750,000 km^3, respectively). The volume of Pliocene–Pleistocene sediments limits the average glacial erosion on the Barents Shelf to be around 650–700 m (1,280,000 km^3/1,900,000 km^2). With the average erosion of 500–700 m in the south (Fig. 2), this calls for a somewhat higher average erosion in the north.

7. Geologic history with quantification of preglacial relief

The rifting of the North Atlantic in Early Tertiary time led to the separation of Greenland and Barents

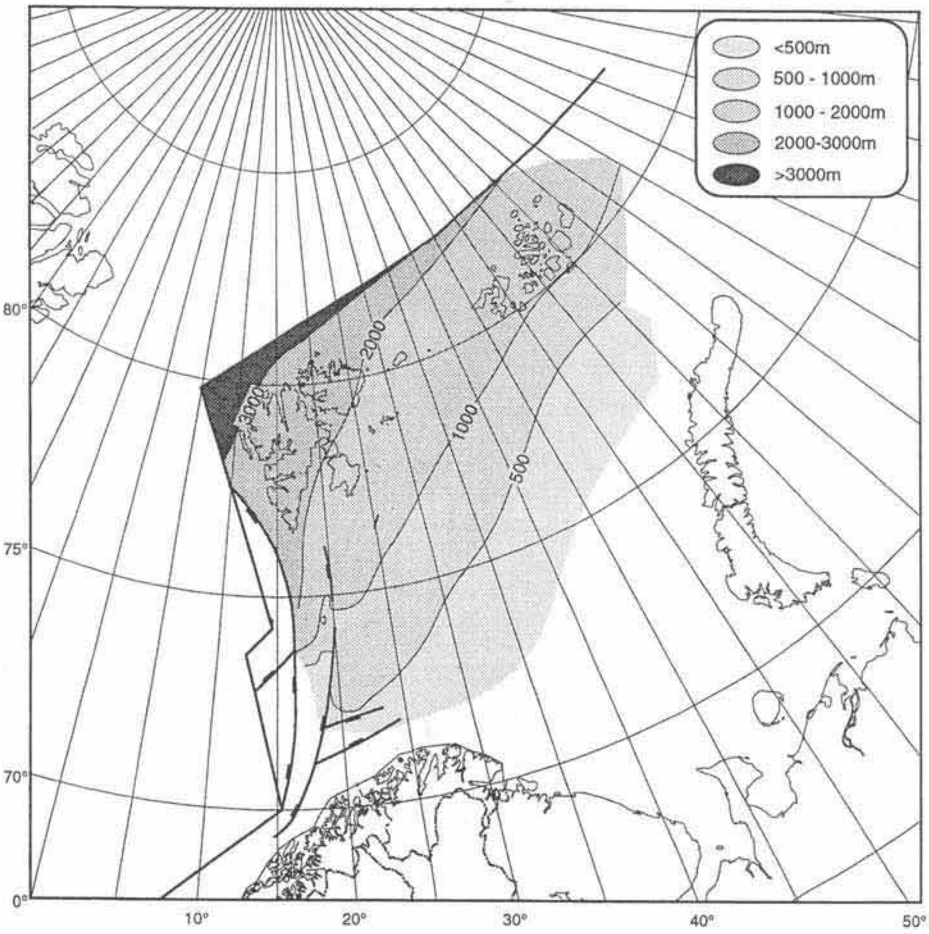

Fig. 6. Reconstructed Early Tertiary postrift topography of the Barents Shelf.

Shelf through complex tectonic phases involving NNW–SSE trending shear movements along the western Barents Sea Margin with final separation and drift in Oligocene times (Talwani and Eldholm, 1977; Myhre and Eldholm, 1988) The tectonic uplift which followed this Early Tertiary rifting is even today topographically expressed by the presence of islands along the rifted margins, with Bjornoya in west, Spitsbergen at the NW tip of the Barents Shelf, and Franz Joseph Land to the north (Fig. 1).

The tectonic uplift after continental rifting is reported to be in the order of 2 km along rifted margins, with asymptotic drop off to less than 500 m uplift some 400–600 km from the margin (Weissel and Karner, 1989). A tentative topographic reconstruction of the Barents Shelf using tectonic uplift of this magnitude is presented in Fig. 6. On Spitsbergen, where a combined uplift effect from both the western and northern margin is to be expected, the maximum uplift in our model is set to 3 km. The tectonic uplift created in this manner is thought to have affected the whole northwestern Barents Shelf, gradually declining to zero towards the sedimentary basins on the southern and southeastern Barents Shelf. This tectonically controlled uplifted land area on most of the NW shelf area was throughout the Eocene, Oligocene to Miocene periods the site of extensive sub aerial erosion, feeding sediments both to the northern and western shelf margin, and also to the basinal areas on the southern and eastern Barents shelf, where most of these soft sediments later were eroded by glacial processes.

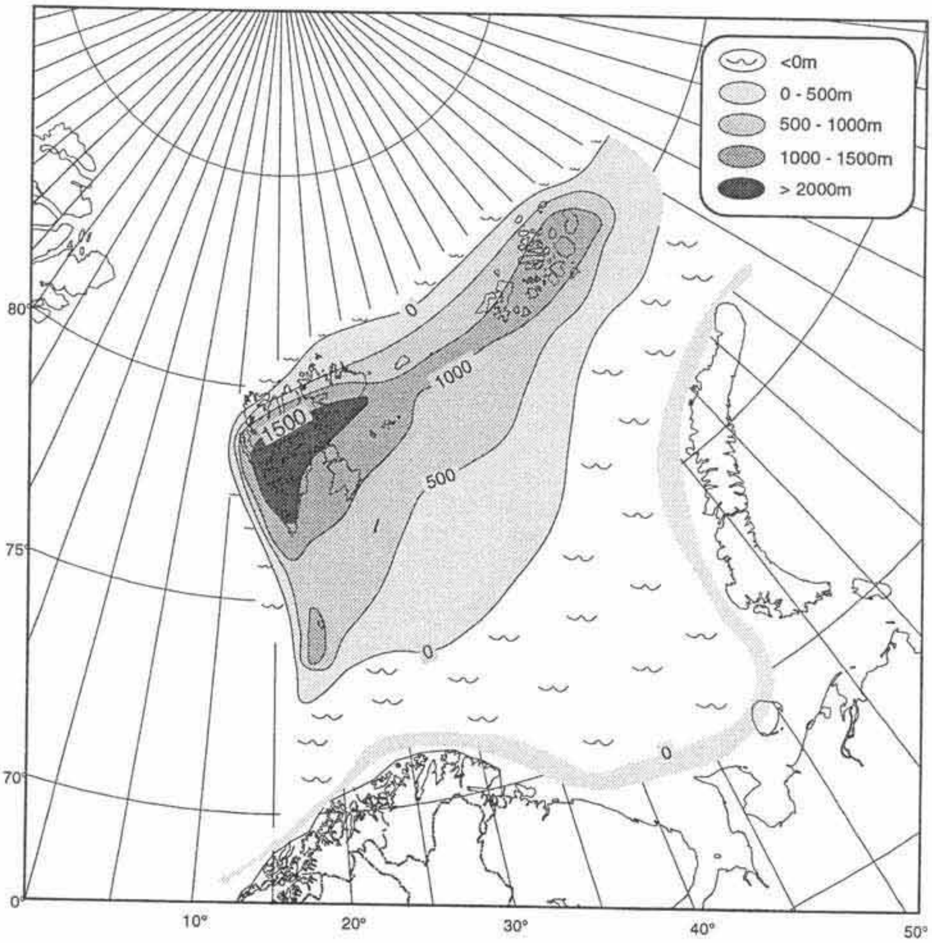

Fig. 7. Reconstructed preglacial relief of the Barents Shelf.

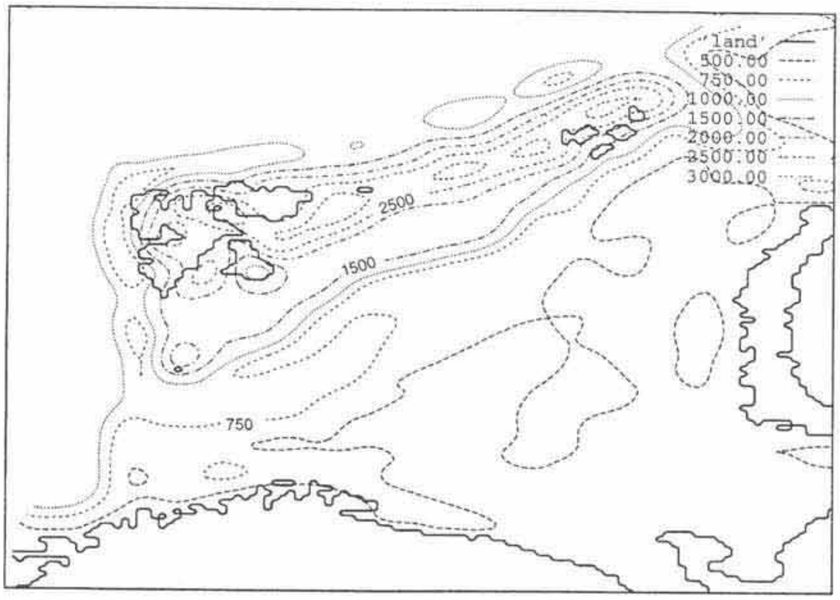

Fig. 8. Estimated amount of eroded Pre-Quaternary sediments using an elastic thickness t_e = 10 km.

In our models, this positive relief on the whole northwestern Barents shelf—with an areal extent of 700,000 km^2—is the major provenance area for the 950,000 km^3 of Early Tertiary sediments as displayed on Fig. 5. Simple volume calculations show that an average depth of erosion of 1200–1300 m over this whole area corresponds to the depositional volumes as calculated above. If the eroded sediments —which mostly will be Late Mesozoic unconsolidated sediments—have an average density of 2000

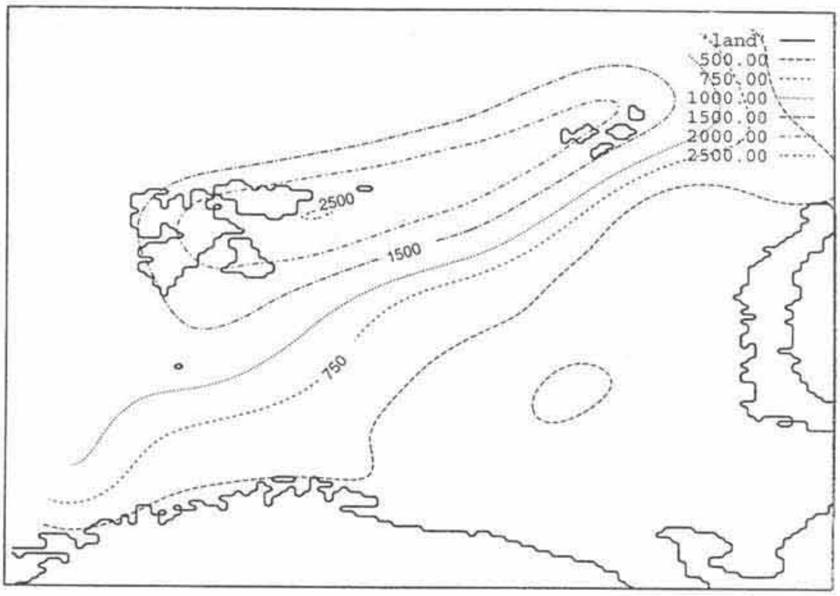

Fig. 9. Estimated amount of eroded Pre-Quaternary sediments using an elastic thickness t_e = 50 km.

kg/m^3, this gives, after isostatic reconstruction (Eq. 2), a 450–500 m lower relief on the whole NW Barents Shelf prior to the glaciations. A tentative preglacial relief is then reconstructed by subtracting 500 m from the Early Tertiary tectonically uplifted northwestern shelf (Fig. 6). A further smoothing of the northwestern most strongly uplifted corner of Svalbard is also introduced to arrive at the tentative pre-glacial relief of the Barents shelf as presented in Fig. 7.

With the present day topography and bathymetry, the preglacial relief is then used to calculate the glacial erosion by using the general equations for isostatic rebound as presented in Eq. 2. Regional maps displaying the glacial erosion for different values of the flexural rigidity are presented in Figs. 8 and 9. For a thin lithosphere ($t_e = 10$ km) the total estimated erosion is seen to have a pronounced local maximum in the Bjornoyrenna, between 750 and 1000 m. The regional maximum occurs in a zone from Spitsbergen to Franz Joseph's Land, where the erosion is estimated to more than 2500 m. For a thick lithosphere ($t_e = 50$ km) the pattern of the estimated erosion is more smeared out, with gradually increasing values from south to north, without any local maximum in the Bjornoyrenna. The maximum erosion is still located in a zone from Spitsbergen to Franz Joseph Land, where 2000 m of erosion is predicted. The total volume of eroded material in the two cases is, however, not very different in the two cases. Planimetering of this erosional map gives a total of 1,200,000 km^3 of eroded material, which agrees with the 1,280,000 km^3 found in sedimentary wedges along the western and northern Barents Shelf Margin.

8. Net uplift

The net uplift of the crust can be estimated from the equation:

$$U(k_x,k_y) = \frac{S(k_x,k_y)\rho_s + H(k_x,k_y)\rho_w + Q(k_x,k_y)\rho_q}{\alpha(k_x,k_y)\rho_m}$$

The erosion pattern described above, combined with the Quaternary deposition and present day bathymetry gives a net uplift of the pre Pliocene–Pleistocene sediments in the order of 400 m in the Bjornoyrenna, and 200–300 m in central Barents Sea. The uplift in the Svalbard area is slightly above 1700 m (Fig. 10).

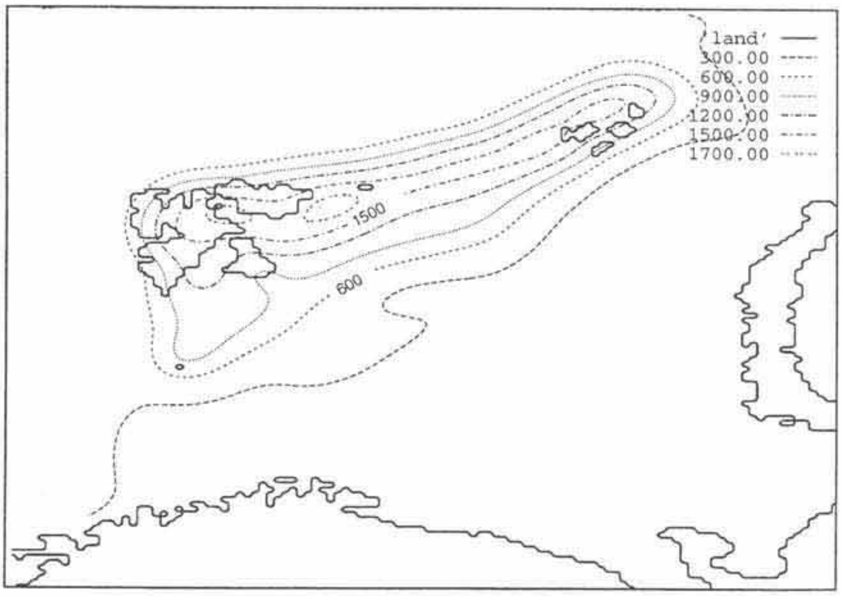

Fig. 10. Estimated net uplift of Pre-Quaternary sediments using an elastic thickness $t_e = 10$ km.

9. The effect of intraplate stress

Could intraplate stresses give a significant modification of this picture? The application of an in-plane force to a lithosphere containing a pre-existing deflection will alter the distribution of bending stresses in the lithosphere, which in turn induces an additional deflection of the lithosphere. An analogue for the lithosphere is a thin elastic plate overlying an inviscid substrate. The thin elastic plate is characterised by its flexural rigidity D, or equivalently by its thickness t_e which we believe represents the mechanically strong part of the lithosphere in a depth-averaged sense.

It has been suggested (e.g. in Cloetingh and Kooi, 1989) that stress-induced subsidence/uplift in rifted basins could be a significant effect in basin formation.

Karner et al. (1993) have shown that the additional deflection, caused by the in-plane force, is simply a filtered version of the pre-existing deflection. The additional deflection caused by the lateral force/unit length N and the pre-existing deflection W_0 in wave number domain (k) is:

$$W_1(k) = \frac{Nk^2}{\Delta\rho_2 g}\left[1 + \frac{(Dk^2 - N)k^2}{\Delta\rho_2 g}\right]^{-1} W_o(k) \quad (3)$$

or equivalently:

$$W_1(k) = \Phi(k) W_o(k)$$

where D is the flexural rigidity, $D\rho_2$ is the density difference between the material underlying and overlying the elastic beam (= mantle density) and g is acceleration due to gravity. Wave number k is related to the wavelength λ by $k = 2\pi/\lambda$.

10. Resulting deflections

The compressional stress field in northern/central Atlantic is suggested to have a magnitude in the order of 3 kbar ($= 0.3 \times 10^{13}$ Nm^{-1}) (Cloetingh and Kooi, 1989). We have used a in-plane compression of 10^{13} Nm^{-1} in east–west direction. Under the assumption of a flat surface (and lithosphere) in Early Pliocene, the deflections caused by the flexural pattern of Fig. 10 can be calculated by Eq. 3. The results for an effective lithosphere thickness of t_e = 10 km ($D = 10^{22}$ Nm) are shown in Fig. 11. It is quite clear that for realistic values of compressional stress in northern Atlantic (note that the compressional stress value used here is three times higher than what is suggested for northern/western Atlantic) the effect of intraplate stresses is insignificant

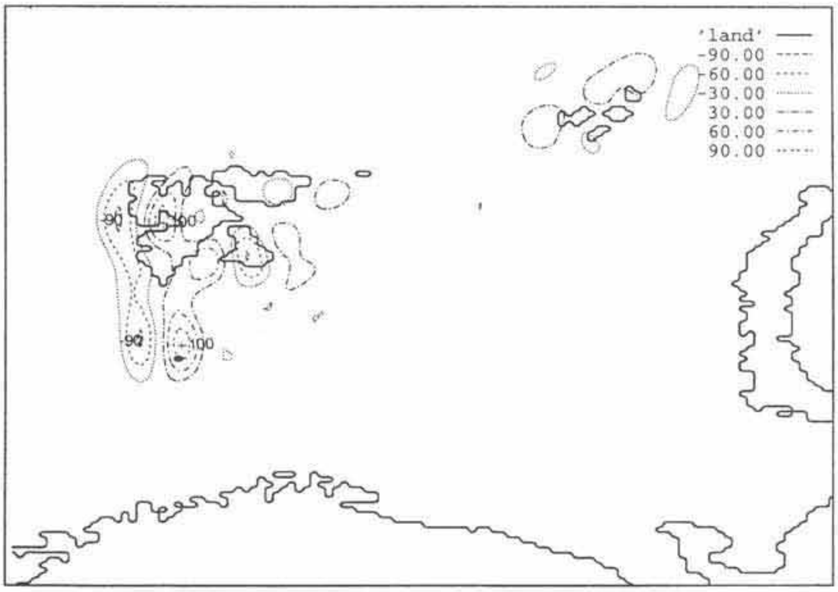

Fig. 11. Deflections due to in-plane force variations on the flexural pattern of Fig. 10. The compression magnitude is 10^{13} Nm^{-1}.

for the overall magnitude of uplift. The deflections have short wavelengths, and the maximum additional deflection caused by the intraplate stress is 100 m close to Svalbard.

We would, however, like to add that the assumption of a horizontal crust with uniform effective thickness in Early Pliocene time is not exactly correct. The lithosphere has been stretched and loaded leading to a non-flat shape of the lithosphere. To give a correct estimate of the effect of the intraplate stress, it is necessary to find the total pre-existing deflection, i.e. take into account the distribution of the entire crustal and sedimentary load. Our assumption about a uniform elastic thickness can also be questioned. In this paper we have taken into account only the load of the Plio/Pleistocene sediments. This error will, however, not affect the results about the wavelength of the uplift. For an elastic thickness of 10 km, the wavelengths of stress induced movements are too short to contribute to the broad scale Barents Sea uplift. As shown in Eq. 3 the stress-induced deflections are a function of the flexural rigidity. $\Phi(k)$ is an effective high-pass filter, removing the components of long wavelengths. Increasing the flexural rigidity increases the filter effect, in addition to removing the components of short wavelengths as well (Fig. 12). For an elastic lithosphere thickness of 10 km the stress induced deflections can be up to 38% of the pre-existing deflections for wavelengths of 100–150 km. For an elastic thickness of 50 km the stress induced deflections have a maximum of 2.8% of the pre-existing deflections at wavelengths of 450 km.

11. Discussion and conclusions

We have attempted to quantify the Tertiary and Quaternary erosion on the Barents Shelf in a two step model:

(1) tectonically related uplift in the order of 500–2000 m and locally 3000 m of the NW Barents Shelf in Early Tertiary times with subsequent erosion in the Eocene–Miocene period with transport of 950,000 km^3 of erosional products to the sedimentary basins on the southern and eastern Barents Shelf and to the continental margins to the west and north.

(2) strongly enhanced erosion in the glacial period with erosion in the magnitude of 1000 m to locally 2000 m on the northern shelf, and 500–700 m on the southern Barents Shelf, and with transport of 1,250,000 km^3 of erosional products to the present-day continental margins to the north and west.

Flexural modelling based on the present day bathymetry in the southern Barents Sea and on anticipated preglacial relief on the northern Barents Shelf,

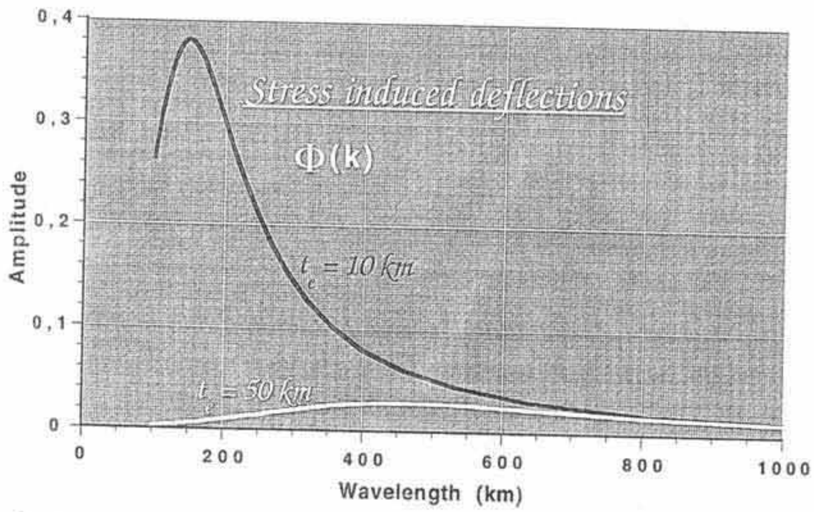

Fig. 12. Deflections as a function of wavelengths due to in-plane force variations ($F(k)$ in Eq. 3) for a thin ($t_e = 10$ km) and a thick ($t_e = 50$ km) elastic lithosphere. The compression magnitude is 10^{13} Nm^{-1}.

gives erosional estimates that accounts for the Pliocene–Pleistocene volumes observed along the present day margins of the Barents Shelf.

Added together this results in a total Tertiary to Quaternary erosion of 2500–3000 m on Svalbard, an estimate in generally good agreement with previous estimates based on published maturation studies of coal (Manum and Throndsen, 1978) and on unpublished Norsk Hydro data of maturation level of Tertiary and Mesozoic shales and mudstones. On the southern Barents Shelf, our estimates of the total Tertiary erosion will be in the range of 500–700 m, an estimate somewhat lower than earlier published estimates (Nyland et al., 1992; Vågnes et al., 1992), although revised maturation studies of the organic rich Jurassic source rocks by using a young Pliocene–Pleistocene erosion shows that these low erosion estimates are possible (J.H. Augustson, Norsk Hydro, pers. comm.).

Our estimates, modelling work and results are weakened by a number of uncertainties, both related to lack of geologic data on large part of the Barents Shelf and sometimes to poor control on input parameters in our equations, which have forced us to make assumptions. Large uncertainties in mapping of the volumes of erosional products north of the Barents Shelf may significantly influence our erosional estimates. Larger volumes will of course result in higher erosion on the shelf. Also our reconstruction of the preglacial relief is totally model driven, and based on an interplay between Early Tertiary tectonic uplift and later Tertiary preglacial erosion. Density of the eroded material is also an important input parameter in our equations. We have used an average of 2200 kg/m^3, which is realistic when we know that the measured Pre-Quaternary bed rock density from exploration wells varies from 2000 kg/m^3 in the southern Barents Sea where the erosion generally is low, up to 2400 kg/m^3 in the northernmost wells where the erosion is proven by various methods to be higher. We have further assumed in our modelling that the preglacial water depth on the southern Barents Shelf was close to 0 m. This is based on the knowledge of a large sediment supply area on the northwestern Barents Shelf which not would allow deepwater sedimentary basins to be stable on the southern Barents Shelf, and to our assumption that the global preglacial sea level is similar to today's level. Vågnes et al. (1992) pointed out that a 200 m of sea level fall in Oligocene would add 600m to the estimated erosion. However, we find no evidence for adding this amount of erosion to our estimates, simply because there is no evidence for such a high additional erosion considering the volumes of the erosional products along the present day margins.

The generally good agreement between our modelled erosion on the shelf and the erosional volumes mapped along the present shelf margin, proves that our method must be treated on line with most other methods as a tool in estimating the erosion on the Barents Shelf.

References

Barton, P. and Wood, R., 1984. Tectonic evolution of the North Sea basin: crustal stretching and subsidence. Geophys. J. R. Astron. Soc., 79: 987–1022.

Brotchie, J.F. and Silvester, R., 1969. On crustal flexure. J. Geophys. Res., 74: 5240–5252.

Caldwell, J.G. and Turcotte, D.L., 1979. Dependence of the thickness of the elastic lithosphere on age. J. Geophys. Res.

Cathles, L., 1975. The Viscosity of the Earth's Mantle. Princeton Univ. Press, New Jersey, 386 pp.

Cloetingh, S. and Kooi, H., 1989. Tectonic subsidence and sea-level changes. In: J. Collinson (Editor), Correlation in Hydrocarbon Exploration. Nor. Pet. Soc., Graham and Trotman, London, pp. 3–11.

Eidvin, T. and Riis, F., 1989. Nye dateringer av de tre vestligste borehullene i Barentshavet. Resultater og konsekvenser for den tertiære hevingen. NPD Contrib., 27, Norwegian Petroleum Directorate, Harstad.

Faleide, J.I., Solheim, A., Fiedler, A., Gjelstuen, B.O., Andersen, E.S. and Vaneste, K., 1996. Late Cenozoic evolution of the Western Barents Sea–Svalbard continental margin. Global Planet. Change, 12: 53–74.

Fiedler, A. and Faleide, J.I., 1996. Cenozoic erosion and sediment yield in the Bear Island fan drainage area. Global Planet. Change, 12: 75–93.

Fjeldskaar, W. and Cathles, L., 1991. Rheology of mantle and lithosphere inferred from post-glacial uplift in Fennoscandia. In: R. Sabadini, K. Lambeck and E. Boschi (Editors), Glacial Isostasy, Sea-Level and Mantle Rheology. Kluwer, Dordrecht, pp. 1–19.

Fjeldskaar, W. and Pallesen, S., 1989. The application of a viscoelastic lithosphere model to isostatic subsidence in backstripping. In: J. Collinson (Editor), Correlation in Hydrocarbon Exploration. Nor. Pet. Soc., Graham and Trotman, London, pp. 53–59.

Fjeldskaar, W., Prestholm, E., Guargena, C. and Gravdal, N., 1993. Isostatic and tectonic development of the Egersund

Basin. In: T. Doré et al. (Editors), Basin Modelling, Advances and Applications. Elsevier, Amsterdam, pp. 549–562.

Gunn, R., 1943. A quantitative evaluation of the influence of the lithosphere on the anomalies of gravity. J. Franklin Inst., 236: 47–65.

Gunn, R., 1944. A quantitative study of the lithosphere and gravity anomalies along the Atlantic Coast. J. Franklin Inst., 237: 139–154.

Jeffreys, H., 1959. The Earth, its Origin, History and Physical Constitution. Cambridge Univ, Press, 4th ed.

Karner, G.D., Driscoll, N.W. and Weissel, J.K., 1993. Response of the lithosphere to in-plane force variations. Earth Planet. Sci. Lett., 114: 397–416.

Kristoffersen, Y., 1990. Eurasia Basin. In: A. Grantz, L. Johnsen and J.F. Sweeney (Editors), The Arctic Ocean Region (Geol. North America, 50). Geol. Soc. Am., Boulder, CO.

Manum, S.B. and Throndsen, T., 1978. Rank of coal and dispersed organic matter and its geologic bearing in the Spitsbergen Tertiary. Nor. Polarinst. Årbok, 1977: 159–177.

Myhre, A.M. and Eldholm, O., 1988. The Western Svalbard Margin. Mar. Pet. Geol., 5.

Nyland, B., Jensen, L.N., Skagen, J., Skarpnes, O. and Vorren, T., 1992. Tertiary uplift and erosion in the Barents Sea: magnitude, timing and consequences. In: R.M. Larsen (Editor), Structural and Tectonic Modelling and its Application to Petroleum Geology. Elsevier, Amsterdam.

Nøttvedt, A., Berglund, T., Rasmussen, E. and Steel, R., 1988. Some aspects of Tertiary tectonics and sediments along the western Barents Shelf. In: A.C. Morton and L.M. Parson (Editors), Early Tertiary Volcanism and the Opening of the NE Atlantic. Geol. Soc. London Spec. Publ., 39: 421–425.

Rasmussen, E., Skott, P.H. and Larsen, K.-B., in press. Hydrocarbon potential of the Bjornoya West Province, Western Barents Sea Margin. Proc. Nor. Pet. Soc. 1992.

Smoluchowski, M., 1909. Versuche über Faltungserscheinungen schwimmender elastischer Platten. Bull. Int. Acad. Sci. Cracovie, pp. 727–734.

Talwani, M. and Eldholm, O., 1977. Evolution of the Norwegian–Greenland Sea. Geol. Soc. Am. Bull., 88.

Vorren, T.O., Lebesbye, E., Andreassen, K. and Larsen, K.-B., 1989. Glacigene sediments on a passive continental margin as exemplified by the Barents Sea. Mar. Geol., 85: 251–272.

Vågnes, E., Faleide, J.I. and Gudlaugsson, S.T., 1992. Glacial erosion and tectonic uplift in the Barents Sea. Nor. Geol. Tidsskr., 72: 333–338.

Vågnes, E., 1996. Cenozoic deposition in the Nansen Basin. A first order estimate based on present day bathymetry. Global Planet. Change, 12: 149–157.

Walcott, R.I., 1970. Flexural rigidity, thickness and viscosity of the lithosphere. J. Geophys. Res., 75: 3941–3954.

Watts, A.B., 1978. An analysis of isostasy in the world's oceans. 1. Hawaiian–Emperor seamount chain. J. Geophys. Res., 83: 5989–6004.

Weissel, J.K. and Karner, G.D., 1989. Flexural uplift of rift flanks due to mechanical unloading of the lithosphere during extension. J. Geophys. Res., 94(B10).